Structural Eng./Earthquake Eng., JSCE, Vol. 18, No. 2, 105s—110s, 2001 July
(J. Struct. Mech. Earthquake Eng., JSCE, No. 682/ I —56)

TWO DIMENSIONAL LAGRANGIAN PARTICLE FINITE DIFFERENCE METHOD FOR MODELING LARGE SOIL DEFORMATIONS

Kazuo KONAGAI[1] and Jörgen JOHANSSON[2]

[1]Member of JSCE, Dr. Eng., Professor, Institute of Industrial Science, University of Tokyo.
(4-6-1 Komaba, Meguro-Ku, Tokyo 153-8505, Japan)
[2]Ph. D., Candidate, Institute of Industrial Science, University of Tokyo.
(4-6-1 Komaba, Meguro-Ku, Tokyo 153-8505, Japan)

LPFDM (Lagrangian Particle Finite Difference Method) is presented for analyzing large deformations of soils. The explicit time-marching solution scheme of LPFDM, in which no global matrix is formed, reduces the computational time considerably. All Lagrangian parameters calculated at each time step are carried by Lagrangian points, which, as a cluster, describe a mass of the material. The updated Lagrangian parameters are then mapped back, for the next calculation cycle, on the stationary Eulerian lattice. LPFDM is thus viewed as an Eulerian way of describing solid motions (LPM, Sulsky et al.[1]) obtained through the *Fast-Lagrangian* scheme of calculation (FLAC, Cundall[2]), and retains the merits of both FLAC and LPM.

Key Words : *large strain of soil, Lagrangian particle method, Eulerian lattice*

1. INTRODUCTION

A number of devastating earthquakes took tragically place in rapid succession in 1999, the closing year of the International Decade for Natural Disaster Reduction (IDNDR). Among them, the earthquakes in Kocaeli, Turkey Aug. 17 and Chi-Chi, Taiwan Sept. 21 were extraordinary. One of the most spectacular aspects of these earthquakes was the fault-inflicted damage to structures. Faultings are not the sole cause of large deformations of soils. Kobayashi found that more than half of all deaths in large ($M > 6.9$) earthquakes in Japan between 1964 and 1980 were caused by landslides. To discuss plausible remedial measures, it is necessary to study the possible extent of the very large plastic deformations taking place in soils. For such studies, suitable numerical tools are needed.

For studying large deformations of soils, numerical methods as FEM or FDM have been widely used. For example, the finite difference based FLAC (Fast Lagrangian Analysis of Continua; Cundall[2]) successfully calculates large strains by using low-order strain elements. The explicit finite difference formulation of FLAC makes it ideally suited for modeling geomechanical problems that often consist of several stages of construction. However, for highly distorted elements, strains are not accurately computed. This is not a problem specific to FLAC. Large element distortions have to be accounted for when dealing with large strains also in e.g. Lagrangian FEM codes

In the field of computational fluid dynamics, where history-dependent materials are less common, purely Eulerian methods are often used. However, to model highly distorted flows, Harlow et al.[3] introduced a partially Lagrangian method, PIC (Particle-In-Cell method). Unfortunately it had high numerical dissipation, and to avoid this problem, Brackbill et al.[4), 5] developed a fully Lagrangian method, FLIP (FLuid Implicit Particle). Not only does it use particles to model convection as in PIC, but it was also extended to model the fluid during the whole calculation cycle. Later, Burgess et al.[6] included a global consistent mass matrix into the FLIP method to reduce the so called "ringing" instability and Sulsky et al.[1] extended it further to solid mechanics. The method is now referred to as the Lagrangian Particle Method (LPM) or the Material Point Method (MPM). In LPM particles

move through the cells of a computational mesh carrying all the necessary Lagrangian parameters such as mass, stress, strain, position, strength etc. Any mesh type could be chosen to suit the typical problem, but a fixed Eulerian mesh is the simplest. The method thus takes advantages of both Eulerian and Lagrangian features, by avoiding mesh distortion and convection problems.

LPFDM (Lagrangian Particle Finite Difference Method) presented herein is intended to be a projection of FLAC formulations on the LPM scheme so that the present method allows for extremely large deformations of soils retaining the merits of FLAC.

2. CALCULATION SCHEME

LPFDM embodies an explicit time-marching scheme, while implicit, matrix-oriented solution schemes are more common in finite element methods. As mentioned, all Lagrangian variables are carried by unconnected Lagrangian material points (see **Fig. 1**); the points, as an entire cluster, describe the mass of the material. A Eulerian mesh is used to solve the equations of motion in each time step. Data mapped from the material points in one cell of the mesh contribute to cell's nodes, and accelerate them. The material points' variables are updated with mesh solution.

For the mesh solution, conventional FLAC[2] uses an overlay scheme, in which a quadrilateral element is modeled as two overlaid pairs of constant-strain triangles (Mixed discretization procdure; Marti and Cundall[7]). The forces exerted on each node are taken to be the mean of those exerted by the two quadrilaterals, and strains are eventually smeared over the quadrilateral. The overlay scheme thereby ensures isotropy, and successfully restrains hourglass deformations. The procedure, however, is not appropriate especially when the quadrilateral is badly distorted and paired triangles' areas are considerably out of balance. As contrasted with FLAC, hourglass deformations do not occur in LPFDM simulations because a fixed Eularian grid is used; hence the overlay scheme is not used in LPFDM allowing strains to be more rationally computed by simply invoking the Gauss' divergence theorem. For an area A enclosed by a surface S, the Gauss' theorem has the following form in the Cartesian coordinate system as:

$$\int_S n_j u ds = \int_A \frac{\partial u}{\partial x_j} dA \qquad (1)$$

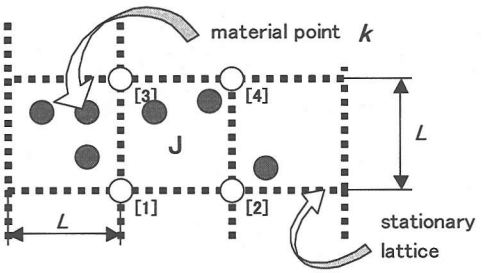

Fig. 1 Stationary lattice and material points

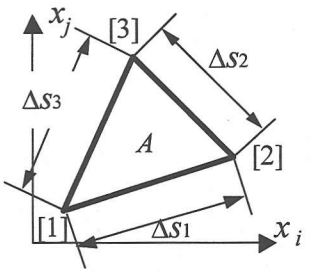

Fig. 2 Triangular cell

where,

$\int_S ds$ is an integral along the boundary S of a closed area A,

n_j $= \mathbf{n} \cdot \mathbf{j}$; Here $\mathbf{n}$ and $\mathbf{j}$ are unit vectors normal to the surface S and along the direction of x_j axis, respectively,

x_j can be either x or y in the Cartesian coordinate system (x, y),

u can be a scalar, vector or tensor, and

$\int_A dA$ is an integral over the area A.

Defining the average value of the gradient over the area as:

$$\left\langle \frac{\partial u}{\partial x_j} \right\rangle = \frac{1}{A} \int_A \frac{\partial u}{\partial x_j} dA \qquad (2)$$

one obtains from Equation (1):

$$\left\langle \frac{\partial u}{\partial x_j} \right\rangle = \frac{1}{A} \int_S n_j u ds \qquad (3)$$

When the closed area is a triangle as shown in **Fig. 2**, and u is assumed to vary linearly along each side, the following finite difference formula is obtained:

$$\left\langle \frac{\partial u}{\partial x_j} \right\rangle = \frac{1}{A} \sum_{k=1}^{3} \langle u \rangle_k n_j \Delta s_k \qquad (4)$$

where, the summation is taken over the three sides, and $\langle u \rangle_k$ is the average value of u over the side k. Keeping in mind that $n_j \Delta s_k$ is the projection of Δs_k on x_i axis, Equation (4) for the triangle in **Fig. 2** is rewritten as:

$$\left\langle \frac{\partial u}{\partial x_j} \right\rangle = \frac{1}{A}\{\frac{u^{[1]}+u^{[2]}}{2}\cdot(x_i^{[1]}-x_i^{[2]})+ \frac{u^{[2]}+u^{[3]}}{2}\cdot(x_i^{[2]}-x_i^{[3]})+\frac{u^{[3]}+u^{[1]}}{2}\cdot(x_i^{[3]}-x_i^{[1]})\} \quad (4a)$$

or

$$\left\langle \frac{\partial u}{\partial x_j} \right\rangle = \frac{1}{2A}\left\{u^{[1]}\left(x_i^{[1]}-x_i^{[2]}\right)+u^{[2]}\left(x_i^{[2]}-x_i^{[3]}\right)+u^{[3]}\left(x_i^{[3]}-x_i^{[1]}\right)\right\} \quad (4b)$$

with $$A=\frac{1}{2}\begin{vmatrix}1 & x_i^{[1]} & x_j^{[1]}\\ 1 & x_i^{[2]} & x_j^{[2]}\\ 1 & x_i^{[3]} & x_j^{[3]}\end{vmatrix}$$

where, superscripts [1], [2], [3] denote local nodal point numbers in **Fig. 2**.

Equation (4) can be used for any arbitrarily-shaped polygon to describe the strain increments in terms of the nodal displacement increments by simply replacing u with $\Delta u^{[k]}$. In LPFDM, a regular square mesh with sides parallel to x and y axes of the Cartesian coordinate system is used (**Fig. 1**). Replacing in Equation (4b) x_i and x_j with x and y, and increasing the node number to four, the average strain increment of J-th element is obtained as:

$$\left(\Delta\varepsilon_{xx}\right)_J = \frac{\left(\Delta u_x^{[2]}+\Delta u_x^{[4]}-\Delta u_x^{[1]}-\Delta u_x^{[3]}\right)_j}{2L} \quad (5a)$$

$$\left(\Delta\varepsilon_{yy}\right)_J = \frac{\left(\Delta u_y^{[3]}+\Delta u_y^{[4]}-\Delta u_y^{[1]}-\Delta u_y^{[2]}\right)_j}{2L} \quad (5b)$$

$$\left(\Delta\varepsilon_{xy}\right)_J = \frac{\left(\Delta u_x^{[3]}+\Delta u_x^{[4]}-\Delta u_x^{[1]}-\Delta u_x^{[2]}\right)_j}{2L} \quad (5c)$$

$$\left(\Delta\varepsilon_{yx}\right)_J = \frac{\left(\Delta u_y^{[2]}+\Delta u_y^{[4]}-\Delta u_y^{[1]}-\Delta u_y^{[3]}\right)_j}{2L} \quad (5d)$$

where L is the cell side length.

The representative shear strain increment $\Delta\gamma_{xy}$ satisfies:

$$\left(\Delta\gamma_{xy}\right)_J = \left(\Delta\varepsilon_{xy}\right)_J + \left(\Delta\varepsilon_{yx}\right)_J \quad (5e)$$

and the corresponding rotational increment $\Delta\theta$ is given by:

$$\left(\Delta\theta\right)_J = \frac{1}{2}\left(\Delta\varepsilon_{yx}-\Delta\varepsilon_{xy}\right)_J \quad (5f)$$

All material points included in Cell J are assumed to experience the same strain increments given by equations (5a)-(5f), and the stresses for a material point k included in Cell J are computed by means of a specified constitutive model:

$$\left(\sigma_{ij}\right)_{k,\,updated} = M\left(\left(\Delta\varepsilon_{ij}\right)_J, \left(\sigma_{ij}\right)_k, \left(s_1\right)_k, \left(s_2\right)_k, \cdots\right) \quad (6)$$

where, $M(\,)$ is the constitutive model, and $\left(s_i\right)_k$ are state variables for this material point. For the explicit scheme used in LPFDM, the constitutive law is only consulted once per material point during one time step.

The location of material point k $\{x(k), y(k)\}$ in the cell J deformed at the previous time step is updated as:

$$x(k) \Leftarrow x(k)+\left(\Delta\varepsilon_{xx}\right)_{k\in j}\cdot\Delta x(k)+\left(\Delta\varepsilon_{xy}\right)_{k\in j}\cdot\Delta y(k)+\left(\Delta u_x^{[1]}\right)_{k\in j}$$

$$y(k) \Leftarrow y(k)+\left(\Delta\varepsilon_{yy}\right)_{k\in j}\cdot\Delta y(k)+\left(\Delta\varepsilon_{yx}\right)_{k\in j}\cdot\Delta x(k)+\left(\Delta u_y^{[1]}\right)_{k\in j} \quad (7a), (7b)$$

where,

$\Delta x(k)$= $x(k)$ - (x-coordinate of node (1) of Cell J)

$\Delta y(k)$= $y(k)$ - (y-coordinate of node (1) of Cell J).

When all the Lagrangian variables are updated at all material points, the equations of motion are solved at each nodes of the Eulerian mesh, which is shifted back to its original position for the following calculation cycle. The mass of each cell is obtained by adding up all the masses of material points included in Cell J:

$$\langle M\rangle_J = \sum_{k\in J} m_k \quad (7)$$

Here, it in noted that a set of material points included in Cell J has been also updated.

Stress is smeared over the cell:

$$\left\langle \sigma_{ij} \right\rangle_J = \left\{\sum_{k\in J}\frac{m_k}{\rho_k}(\sigma_{ij})_k\right\}/L^2 \quad (8)$$

where, the quotient of material point mass and density m_k/ρ_k is the volume of the material point k. In order to obtain the nodal forces at node [k] of Cell J (see **Fig. 1**), a virtual unit displacement is applied to node [k]. The stress components $\langle\sigma\rangle_J$ smeared over Cell J must perform the same amount of work done by the nodal forces $F_i^{[k]}$ ($i = x$ or y): this calls for;

$$F_i^{[k]} = \frac{\langle\sigma_{ii}\rangle_J\left(x_j^{[k-1]}-x_j^{[k+1]}\right)}{2}+\frac{\langle\sigma_{ij}\rangle_J\left(x_i^{[k-1]}-x_i^{[k+1]}\right)}{2} \quad (9)$$

where, $(x_i \quad x_j)$ is either $(x \quad y)$ or $(y \quad x)$.

At each node, the forces from all surrounding lattice zones (elements) are summed up to give the net nodal force, $\sum_{[k]\in(k)} F_i^{[k]}$ ($i = x$ or y). This vector includes contributions from applied loads and body forces due to gravity. Gravity forces are computed from:

$$F_{g,i}^{(k)} = g_i m^{(k)} \tag{10}$$

where $m^{(k)}$ is the lumped mass at the node (k), defined as 1/4 of the masses of the cells connected to the node. If a connected cell does not contain any material point, its contribution to the nodal force is omitted. The nodal force accelerates the lumped mass, and the acceleration is integrated to obtain the nodal displace increment:

$$\Delta u_i^{(k)}(t+\Delta t/2) = \Delta u_i^{(k)}(t-\Delta t/2) + \frac{\Delta t^2}{m^{(k)}} \sum F_i^{(k)} \tag{11}$$

It is noted in Equation (11) that the nodal displacement increment $\Delta u_i^{(k)}(t-\Delta t/2)$ is not exactly identical to that evaluated at the previous time step of the calculation cycle, because the increment must be evaluated at the node on the Eulerian lattice shifted back to its original position while the point where the previous increment was evaluated has passed by this node. Compensation for this is made by the following procedure:

$$\Delta u_x^{(k)}(t-\Delta t/2) \Leftarrow \Delta u_x^{(k)}(t-\Delta t/2)\cdot\left(1-\left(\Delta\varepsilon_{xx}\right)_{J^{(k)}}\right) - \Delta u_y^{(k)}(t-\Delta t/2)\cdot\left(\Delta\varepsilon_{xy}\right)_{J^{(k)}} \tag{12a}$$

$$\Delta u_y^{(k)}(t-\Delta t/2) \Leftarrow \Delta u_y^{(k)}(t-\Delta t/2)\cdot\left(1-\left(\Delta\varepsilon_{yy}\right)_{J^{(k)}}\right) - \Delta u_x^{(k)}(t-\Delta t/2)\cdot\left(\Delta\varepsilon_{yx}\right)_{J^{(k)}} \tag{12b}$$

where, $J^{(k)}$ is the cell in which the previous mark of nodal point (k) on the material is found.

When quasi-static behaviors are concerned, the motions of nodes must be damped with minimal computational effort. A form of artificial damping, called local non-viscous damping (Cundall[2]), is used in LPFDM in which the damping force on a node is proportional to the magnitude of the unbalanced force. The direction of the damping force is taken in such a way that energy is always dissipated. Equation (11) is thus replaced with the following equation:

$$\Delta u_i^{(k)}(t+\Delta t/2) = \Delta u_i^{(k)}(t-\Delta t/2) + \frac{\Delta t^2}{m_k}\left(\sum F_i^{(k)} - D_i^{(k)}\right) \tag{13}$$

where, $D_i^{(k)} = \alpha\left|\sum F_i^{(k)}\right| \mathrm{sgn}(\Delta u_i^{(k)}(t-\Delta t/2))$ (14)

$D_i^{(k)}$ is the damping force, α is a constant.

3. NECESSARY ITEMS

A fixed mesh, in an arrangement of $mx \times my$ square cells with "***nodal points***", is used to describe the locations of "***Lagrangian points***" (**Fig. 3**). Rectangular parts of the lattice filled with Lagrangian points are referred to as "***clusters***". Initially, Lagrangian points are arranged in square in each cell of a cluster.

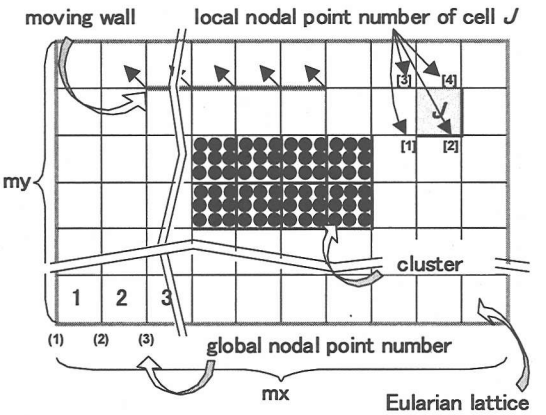

Fig. 3 Necessary items in LFPDM.

In addition to the abovementioned items, "***moving walls***" are introduced into LPFDM. A *moving wall* is realized by giving all designated nodes lined up on the lattice the same displacement increments at once. When the accumulation of the increments given to each node reaches one cell size, the displacement increments are given to the next line of nodes.

4. NUMERICAL EXAMPLES

Lagrangian points discussed herein is assumed to be elasto-plastic, obeying the simple Mohr-Coulomb's yield criterion. Once the peak strength is reached in one intact Lagrangian point, chemical bonds or granular fabrics are assumed to be broken causing the material strength to be reduced from its initial value to some prescribed extent. Both the internal friction angles and the cohesions for Lagrangian points were modified to fluctuate randomly around their mean values so that the deviations eventually exhibit the Gaussian distributions. This manupulation is based on the idea that a material exhibiting a complicated hysterisis is comprised of a number of elements exhibiting simple and ideal features (Iwan[8], Ogawa[9]).

Parameters (mean values) for the material used in the following examples are listed in **Table 1**. Standard deviations of the fluctuated parameters for the following examples were set at 33% of their mean values.

Table 1 Mechanical properties

Young's modulus:	5×10^7 N/m^2
Poisson's ratio:	0.47
Density:	1700 kg/m^3
Internal friction angle:	0.5 rad
Cohesion:	9800 N/m^2
Strength reduction:	Cohesion is reduced by 50%

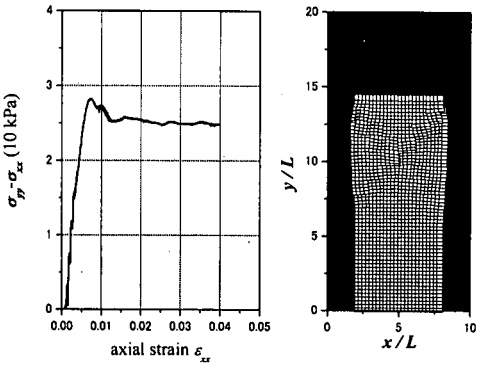

Fig. 4 PSC test simulation
(Cap cluster of stiffer LP is not illustrated)

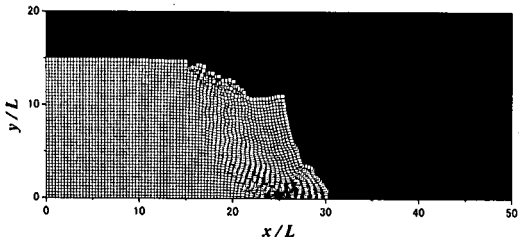

Fig. 5 Simulation of cliff failure ($\Delta t = 0.0001$ s)
(8000 steps after the cliff was put in the gravitational field)

(1) Plane-strain compression test

Fig. 4 shows the simulation of a plane-strain compression test. In order to compress the specimen (a cluster of material points), another cluster of stiffer Lagrangian points, a cap, was put immediately above the top end of the specimen, and was slowly driven down by a "*moving wall*" embedded in the *cap* cluster. The confining pressure was set at zero. In the figure right, both the height and width of the specimen are normalized by the cell width L, and material points are initially arranged in 4×4 square in each cell. Though each material point has a polygonal stress-strain relationship, the overall deviatoric stress-strain relationship exhibits rather gentle curve because the values given in **Table 1** were initialized with random deviation. Two diagonal shear bands can be seen across the specimen.

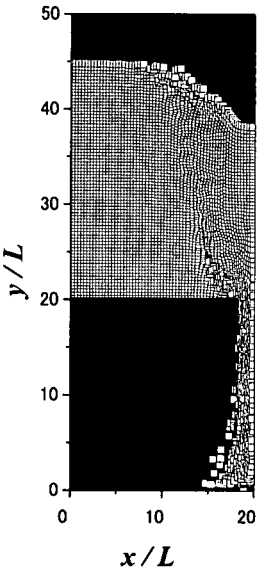

Fig. 6 Mass flow through a trapdoor
($\Delta t = 1 \times 10^{-4}$s, 16000 steps after the flow started)

(2) Failure of cliff

Fig. 5 shows a soil mass that collapses under its own weight. As has been mentioned in Chapter **2**, a form of damping, called local non-viscous damping (Cundall[2]), was used to damp the motion of the cliff material, and α in Equation (14) was tentatively set at 0.8 following the Cundall's example. Despite the coarse discretization ($L = 1$m), detailed features of this cliff failure were vividly described. Initially the deformation is slow, but as plastic strains begin to accumulate, certain regions become softened and rapid shear-band formation occurs. The corner wedge of the soil mass then starts sliding down the softened slope, being followed by some surface Lagrangian points that has come off scarps formed in succession behind the sliding wedge. These Lagrangian points are stopped when their heap makes an angle of repose.

(3) Mass flow through a trapdoor

A mass flow through a trap door was simulated (**Fig. 6**). The gravitational acceleration was given at once to the mass with mechanical properties listed in **Table 1**, and the mass started flowing under its own weight. The opening of the door is just twice the cell size L, and yet, the mass exhibiting a noticeably flexible nature can flow through the narrow opening.

5. CONCLUSIONS

LPFDM (Lagrangian Particle Finite Difference Method) presented herein has a simple LPM scheme, where unconnected Lagrangian material points move across a stationary Eularian lattice and carry all Lagrangian parameters. Data mapped from the Lagrangian points in one cell of the mesh contribute to cell's nodes, and the cell deforms carrying the Lagrangian points. But the cell is then shifted back to its original position for the next calculation cycle. The explicit time-marching scheme for LPFDM is similar to FLAC, and makes the method ideally suited for modeling geotechnical problems. In LPFDM, however, to keep track of large soil deformations is more feasible because a fixed Eularian grid is used and cells are not distorted too excessively. Therefore, demanding formulations for largely distorted elements are not necessary. In the present numerical examples, Lagrangian points were assumed to be elasto-plastic, obeying the simple Mohr-Coulomb's yield criterion. Parameters for this simple bi-linear or polygonal stress-strain relationship were fluctuated randomly from point to point. This might be an oversimplification of reality, but it was based on an idea that a material exhibiting a complicated hysterisis is comprised of a number of elements exhibiting rather simple and ideal features.

To allow for more quantitative discussions, future extensions to the method should include implementation of pore water pressure, and etc. The discussion for this extension will be addressed in a future publication.

ACKNOWLEDGMENT: Partial financial supports for this study have been provided by the Japan Society for the Promotion of Science (Grant-in-Aid for Scientific Research, No. 11875101 and 12355020).

REFERENCES

1) Sulsky, D., Chen, Z. and Schreyer, H. L.: A particle method for history dependent materials, *Comput. Methods Appl. Mech. Engrg.*, Vol. 118, pp. 179-196, 1994.
2) Cundall, P.A. and Board, M.: A microcomputer program for modeling large-strain plasticity problems, *Numerical Methods in Geotechnics (Proc., 6th Int. Conf., Innsbruck, Austria, April 1988)*, pp. 2101-2108. 1988.
3) Harlow, F.H.: The particle-in-cell computing method for fluid dynamics in fundamental methods in Hydrodynamics, Alder, B., Fernbach, S. and Rotenberg, M. (Eds.), *Experimental Arithmetics*, Academic Press, pp. 319-345, 1964.
4) Brackbill, J.U. and Ruppel, H. M.: FLIP: A method for adaptively zoned, particle in cell calculations of fluid flows in two dimensions, *Jour., Comput. Phys.*, Vol. 65, pp. 314-343, 1986.
5) Brackbill, J. U., Kothe, D. B. and Ruppel, H. M.: 'FLIP': A low dissipation, particle-in-cell method, *Jour. Comput. Phys.*, Vol. 96, pp. 339-368, 1988.
6) Burgess, D., Sulsky, D. and Brackbill, J. U.: Mass matrix formulation of the FLIP particle in cell method, *Jour. Comput. Phys.*, Vol. 103, pp. 1-15, 1992.
7) Marti, J. and Cundall, P. A.: Mixed discretization procedure for accurate solution of plasticity problems, *Int. Jour., Num. Methods & Analy. Methods in Geomech.*, Vol. 6, pp. 23-26, 1982.
8) Iwan, W.D. : A distributed-element model for hysterisis and its steady-state dynamic response, *Jour., Appl. Mechanics*, pp. 893-900, 1966.
9) Ogawa, Y.: A model for hysterisis of soil and its steady-state strain energy and energy loss, *Proc., 6th Japan Earthquake Engineering Symp.*, pp.529-536, 1982.

(Received August 28, 2000)

地盤の大変形解析のための 2次元ラグランジアン・ポイント有限差分法

小長井 一男・ Jörgen JOHANSSON

地盤の大変形解析のためのLPFDM（ラグランジアン・ポイント有限差分法）を提示した．これは有限差分法のスキームでの時刻暦解析法で，全体マトリックスを構築する必要がない．解析対象となる物質はラグランジアン・ポイントと呼ばれる点の集合で表現される．1回のタイムステップで更新されたラグランジアン パラメータ（点の座標値なども含む）はバックグランドであるEuler座標上にマッピングされ，次のステップの計算に移行する．したがって，本手法はSulskyらが開発したラグランジアン・ポイント法(LPM)にFLACなどと共通する有限差分法のスキームを反映したもので，両者の特徴を反映し，大変形解析を，少ない計算負荷で行うことを可能にする．